Available online at www.sciencedirect.com
ScienceDirect
Journal of Nuclear Materials 367–370 (2007) 864–868
journal of nuclear materials
www.elsevier.com/locate/jnucmat

Retention and desorption behavior of helium in oxidized V–4Cr–4Ti alloy

D. Oku *, T. Yamada, Y. Hirohata, Y. Yamauchi, T. Hino

Laboratory of Plasma Physics and Engineering, Division of Quantum Science and Engineering, Graduate School of Engineering, Hokkaido University, Kita-13, Nishi-8, Kita-ku, Sapporo 060-8628, Japan

Abstract

Retention and desorption behaviors of helium in oxidized and non-oxidized V–4Cr–4Ti alloy samples were investigated after helium ion irradiation at room temperature using a thermal desorption spectroscopy. The ion energy and fluence were 5 keV and $(0.5–10)\times10^{21}$ He/m^2, respectively. An oxidized layer with a thickness of 100 nm was prepared by thermal oxidation. The surface density of blisters produced by helium ion irradiation in the oxidized sample was lower than that in the non-oxidized one. The helium desorption behavior depended significantly on the fluence. In the lower fluence regime, the retained helium desorbed mainly at around 1300 K in both samples. As fluence increased, several desorption peaks appeared in the low temperature region in both samples. However, the peak temperatures were different. The amount of helium retained in the oxidized sample was lower than that in the non-oxidized sample.

1. Introduction

Vanadium alloy is a candidate material as first wall and structural materials in a fusion reactor, owing to its low induced radioactivity and good thermal and mechanical properties at high temperature [1–5]. This alloy showed excellent mechanical tolerance to neutron damage [2,3], and low helium and hydrogen production rates due to 14 MeV neutron irradiation [5]. For a high tritium breeding ratio, it is desirable not to attach armor to the first wall of a vanadium blanket structure. In this case, the first wall is exposed directly to fusion plasmas, including helium ions. In addition, the V-alloy is exposed to helium glow discharges employed for wall conditioning such that it is irradiated by He ions with different energies. In a previous study, it was found that many blisters were formed on the surface of vanadium alloy after helium ion irradiation with high ion fluence at low temperature [6–8]. If the blisters and internal bubbles are formed, the retained helium reemits into the plasma and then fuel dilution may take place. Thus, it is required to investigate the retention and desorption behavior of helium.

The helium retention behavior in vanadium and a vanadium alloy irradiated by helium ion has been reported, but the range of ion fluence was low ($\sim10^{18}$ He/m^2) [9–11]. It was also reported that

* Corresponding author. Tel./fax: +81 11 706 6662.
E-mail address: akande@apollo.qe.eng.hokudai.ac.jp (D. Oku).

0022-3115/$ - see front matter © 2007 Elsevier B.V. All rights reserved.
doi:10.1016/j.jnucmat.2007.03.068

impurities enhanced helium retention owing to formation of He_nVX and/or He_nV_mX type defect clusters related to impurity (X) [8,10]. Furthermore, it is well known that the vanadium alloy, as well as vanadium, is easily oxidized [12]. It is therefore possible that the retention and desorption behavior of helium in the oxidized vanadium alloy may differ from that in the non-oxidized vanadium alloy.

In this study, the retention and desorption behavior of helium in a surface oxidized V–4Cr4–Ti alloy was investigated and compared with that of a non-oxidized one.

2. Experiments

Three kinds of samples were prepared for this study. As a starting material, cold-rolled V–4Cr–4Ti samples with low impurity contents [13], NIFS-HEAT-2 prepared by National Institute for Fusion Science (NIFS), was used. The sample size was 40 mm × 5 mm × 0.25 mm. Table 1 shows pre-treatment procedure of each sample used in this study. A cold-rolled sample was annealed at 873 K for 30 min in a vacuum of 10^{-5} Pa by using a vacuum apparatus with an infrared image furnace. This sample is referred to as the 'non-oxidized sample' in this paper. A non-oxidized sample was oxidized under the condition of an oxygen pressure of 0.05 Pa at 873 K (operation temperature of V-alloy blanket) for 15 min. This sample is referred to as 'oxidized sample'. Pre-treatment procedure of 'annealed sample', which was V–4Cr–4Ti sample annealed at 1373 K for 1 h in a vacuum [7,8], is also shown in Table 1 to be compared with the oxidized and the non-oxidized samples.

The depth profiles of atomic composition in the oxidized and the non-oxidized samples were analyzed by using Auger electron spectroscopy, AES, with 3 keV-Ar ion etching.

The helium ion irradiation was conducted at room temperature for both the samples by using an ECR ion irradiation apparatus [14]. An irradiated area is 5×20 mm^2. The energy of helium ion was 5 keV and the flux was approximately 10^{18} He/m^2/s. The fluence was taken in the range from 5×10^{20} to 10^{22} He/m^2, which corresponds to 4.5 dpa at fluence of 5×10^{20} He/m^2 to 91 dpa at fluence of 1×10^{22} He/m^2. This fluence range is comparable with that of α-particles in the operating condition of a DEMO reactor. Here it is noted that the number of displacements per atom was an average value in the ion projected range (27 nm) of 5 keV He ion.

Table 1
Pre-treatment procedure of each sample

Sample name	Pre-treatment procedure	Fluence (He/m^2)
Non-oxidized sample	Annealing (873 K, 30 min, 10^{-5} Pa)	$(0.5–10) \times 10^{21}$
Oxidized sample	Annealing (873 K, 30 min, 10^{-5} Pa) → oxidation (873 K, 15 min, 0.05 Pa)	$(0.5–10) \times 10^{21}$
Annealed sample [7,8]	Annealing (1373 K, 1 h, 10^{-5} Pa)	5×10^{21}

After the irradiation, the desorption behavior and the amount of retained helium were examined in the ion irradiation apparatus using thermal desorption spectroscopy, TDS. The irradiated sample was heated from room temperature to 1600 K with a constant heating rate of 1 K/s. The change of the surface morphology after the ion irradiation was examined using a scanning electron microscope, SEM.

3. Results and discussion

Fig. 1 shows the depth profiles of V, C, and O at the surface region of the non-oxidized sample (a) and the oxidized sample (b). The depth was estimated by using the sputtering yield of pure vanadium of 3 keV Ar ion [15]. The oxygen concentration in the near surface region of the non-oxidized sample was comparable with that of the cold-rolled V–4Cr–4Ti, while the carbon concentration was lower than that of the cold-rolled sample [8]. Compared to the annealed sample [8], the oxygen concentration at the near surface of the non-oxidized sample was higher, while the carbon concentration was roughly the same. The thickness of the oxidized layer in the non-oxidized sample was evaluated to be 18 nm, which is shallower than that of the projected range of 5 keV helium ions (~27 nm).

The oxygen and carbon concentrations in the oxidized sample (Fig. 1(b)) were significantly different to those of the non-oxidized sample. The oxygen concentration was ~65 at.% at the top surface, and exponentially decreased with depth. The oxygen concentration became 1/e of that at the top surface when the depth was about 100 nm. This thickness is approximately four times larger than the projected range of the He ions (27 nm). In addition, this thickness is larger than the sputtered thickness (4.8 nm) due to the helium ion fluence of 5×10^{21} He/m^2. Therefore, the helium ions are implanted in the oxidized layer even if the surface layer is etched by

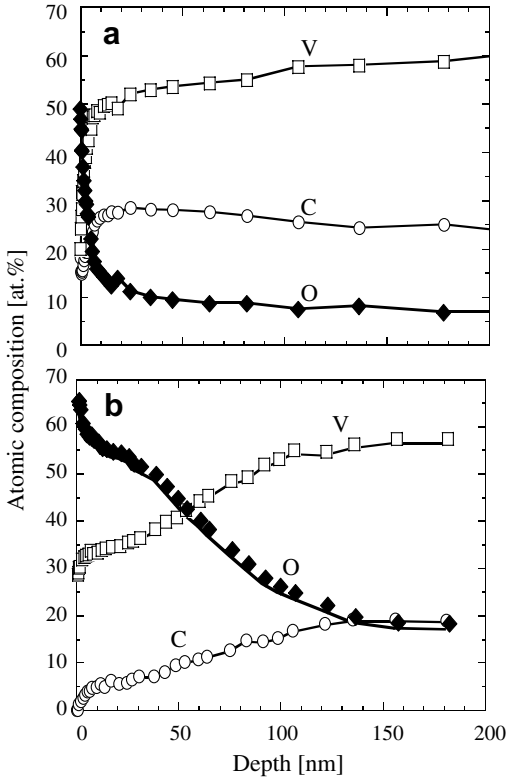

Fig. 1. Depth profile at the surface region in the non-oxidized (a) and the oxidized sample (b).

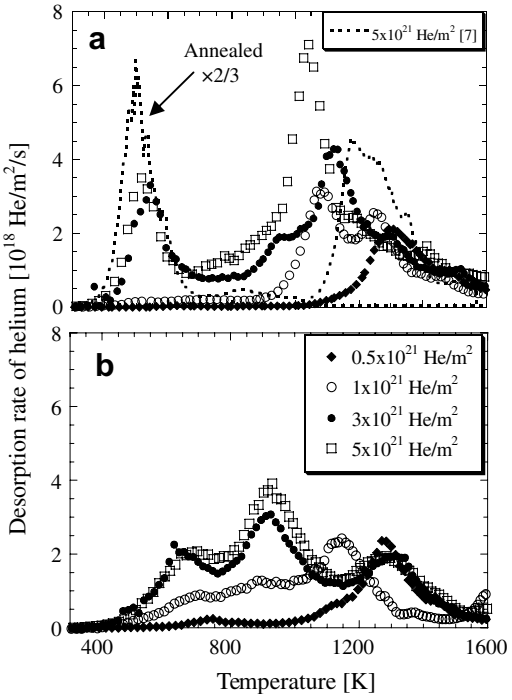

Fig. 2. Thermal desorption spectra of helium in the non-oxidized sample (a) and the oxidized sample (b) after helium ion irradiation at room temperature. Here, dotted line in (a) shows the spectrum in the annealed sample after helium ion irradiation with a fluence of 5×10^{21} He/m^2 [7].

sputtering. The carbon concentration in the oxidized sample was observed to be relatively low. This may have been due to loss of carbon by formation of CO and CO_2 during oxidation.

Fig. 2 shows thermal desorption spectra of helium for the non-oxidized sample (a) and the oxidized sample (b) after the helium ion irradiations with different fluences. In Fig. 2(a), the helium desorption spectrum of the annealed sample after helium ion irradiation with a fluence of 5×10^{21} He/m^2 is also shown by a dotted line. Here, the desorption rate of the annealed sample is scaled down by factor of 2/3. Several desorption peaks were observed in the TDS spectra in the non-oxidized and oxidized samples. The TDS spectra depended on the helium ion fluence, i.e. in the lower fluence region ($<1 \times 10^{21}$ He/m^2), the retained helium mainly desorbed at around 1300 K, and as the fluence increased, several desorption peaks were observed at lower temperatures. The peak temperatures (T_p) in both samples are summarized in Table 2.

The activation energies (E) for the peaks were estimated by using Redhead's equation [16].

$$E = RT\left(\ln\frac{T_p v_1}{\beta} + \ln\frac{1}{\ln\frac{T_p v_1}{2\beta}}\right). \quad (1)$$

Here, R is gas constant, T_p peak temperature and β heating rate ($= 1$ K/s). The frequency (v_1) is assumed to be 10^{13} s^{-1} [16,10]. The activation energies of desorption in the non-oxidized and the oxidized sample are also shown in Table 2. The major desorption peaks of the non-oxidized sample were observed at around ~523, 1085 and 1292 K (Fig. 2(a), Table 2). At the low fluence (0.5×10^{21} He/m^2), the retained helium was mainly desorbed at around 1292 K. However, as the fluence increased, the main desorption peaks were observed at 523 and 1085 K. The desorption peak at 523 K became large as the fluence increased. A similar tendency was observed in the annealed sample [7]. The lower temperature peaks appeared at roughly the same temperatures with the increasing fluence. However, the higher temperature peaks shifted to a little lower temperature as the fluence increased. Higher temperature peaks in the annealed sample did not tend to shift similarly.

Table 2
The desorption peak temperature (T_p) and the activation energies (E) of helium in the non-oxidized sample and the oxidized sample

Traps	Non-oxidized sample			Oxidized sample		
	T_p (K)	E (eV)	I[a]	T_p (K)	E (eV)	I[a]
Defect clusters	**523**	**1.50**	**s**	547	1.57	w
	640	1.85	w	**685**	**1.98**	**s**
	757	2.20	w			
	910	2.66	w	**908**	**2.65**	**s**
Blisters and bubbles	**1085**	**3.18**	**s**	**1125**	**3.30**	**s**
	1210	3.56	w			
	1258	3.71	w	1265	3.73	w
	1292	**3.81**	**s**	**1295**	**3.82**	**s**
				1375	3.06	w
	1464	4.33	w	1431	4.23	w

Traps are main sites retaining helium.
[a] I is intensity of the peaks. s: strong, w: weak.

It has been reported that the dissociation energies of He_nVX type and He_nV_6X type defect clusters for the V and V-alloy were ~1.5 eV and ~2.48 eV, respectively [10]. Here, n is the number of helium atoms ($n > 1$), V vacancy, and X impurity atoms such as C, N, or O. In our previous study, it was found that the desorption in the high temperature region (>1100 K) corresponded to the ruptures of blisters and internal bubbles in the annealed sample (see Fig. 2(a)) [7]. Based on these reports and the activation energies, it is thought that desorption at ~523 K corresponds to the dissociation of He_nVX type defect cluster while the higher temperature (>1100 K) desorption is associated with the rupture of blisters and internal bubbles. However, shift of the higher temperature peaks in the non-oxidized sample, mentioned in preceding paragraph, would be due to changes in the activation energies of blisters and internal bubbles as the fluence increased, or the formation of new traps with different activation energies.

The major desorption peaks in the oxidized sample were observed at 685, 908 and 1295 K (Fig. 2(b), Table 2). One can see that the amount of helium desorbed at ~1295 K, corresponding to the rupture of the blisters and bubbles, saturated at the low fluence (0.5×10^{21} He/m^2), and in the high fluence range ($\geqslant 1 \times 10^{21}$ He/m^2), the desorption peaks at around 685 and 908 K became large. The desorption peaks at 685 and 908 K correspond to dissociation of He_nV_mX ($m > 1$) type defect cluster [10]. These peak intensities were smaller compared with the major peak intensities at 523 and 1085 K in the non-oxidized sample and the annealed sample (Fig. 2(a)) [7].

Fig. 3 shows the total amount of retained helium in the non-oxidized and the oxidized sample as a function of the fluence. In this figure, the amount in the annealed sample is also plotted for comparison. Total amount of retained helium saturated at a fluence of 5×10^{21} He/m^2 in the three samples. The saturation levels of the non-oxidized and the oxidized sample were 2.5×10^{21} He/m^2 and 1.9×10^{21} He/m^2, respectively. The saturation value in the oxidized sample was about 75% of that in the non-oxidized sample, and 70% of that in the annealed sample. These results show that the amount of retained helium in the oxidized alloy is lower compared with that of the non-oxidized alloy.

Fig. 4 shows SEM photographs of the oxidized (a) and the annealed samples (b) after the irradiation with a fluence of 5×10^{21} He/m^2 (45 dpa) [7].

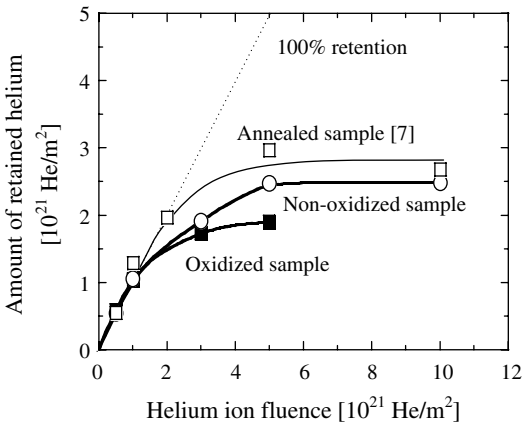

Fig. 3. Total amounts of retained helium in the non-oxidized, the oxidized and the annealed samples as a function of fluence.

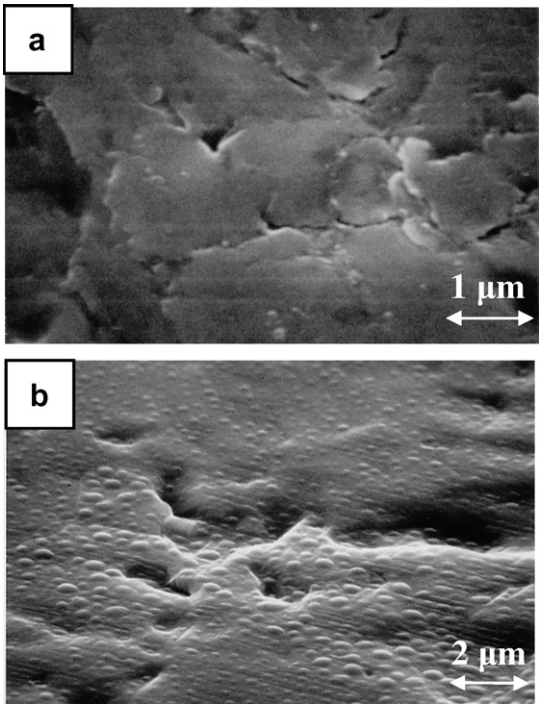

Fig. 4. SEM photographs of the oxidized sample (a) and the annealed sample (b) after helium ion irradiation with a fluence of 5×10^{21} He/m^2 (45 dpa) [7].

Many blisters were observed on the surface of the annealed sample. The size and distribution of the blisters were not uniform (Fig. 4(b)). On the other hand, in the oxidized sample only a few blisters were observed on the surface (Fig. 4(a)) and their size was smaller compared to that in the annealed sample. This result indicates that the amount of retained helium in the oxidized sample is less, consistent with the TDS results.

4. Conclusion

Retention and desorption behavior of helium in the oxidized V–4Cr–4Ti alloy was investigated by using an ECR ion irradiation apparatus, TDS and SEM. After the helium ion irradiation, the desorption peak at around 1300 K appeared in both the oxidized sample and the non-oxidized sample when the ion fluence was relatively low. This helium desorption is probably related to the ruptures of blisters and bubbles. As the ion fluence increased, the desorption peaks in the lower temperature region appeared in both samples. In the non-oxidized sample, the peak temperature was 523 K, and this desorption is most likely due to the dissociation of He_nVX defect clusters. In the oxidized sample, major desorption peaks appeared at temperatures of 680 and 900 K. These desorptions are also regarded as the dissociation of He_nV_mX. The amount of retained helium in the oxidized sample was observed to be smaller than that in the non-oxidized sample due to fewer blisters and/or bubbles. The present results show that the surface oxidation for the vanadium alloy significantly changes the retention and desorption behavior of helium.

Acknowledgements

Authors wish to thank Drs T. Muroga and T. Nagasaka, NIFS, for the supply of V-alloy samples. This study was supported by JSPS KAKENHI(16560719 and 15760619) and the NIFS LHD Project Research Collaboration.

References

[1] H. Matsui, K. Fukumoto, D.L. Smith, Hee M. Chung, W. van Witzenburg, S.N. Votinov, J. Nucl. Mater. 233–237 (1996) 92.
[2] S.J. Zinkle, H. Matsui, D.L. Smith, A.F. Rowcliffe, E. van Osch, K. Abe, V.A. Kazakov, J. Nucl. Mater. 258–263 (1998) 205.
[3] D.L. Smith, H.M. Chung, B.A. Loomis, H.-C. Tsai, J. Nucl. Mater. 233–237 (1996) 356.
[4] T. Muroga, T. Nagasaka, K. Abe, V.M. Chernov, H. Matsui, D.L. Smith, Z.-Y. Xu, S.J. Zinkle, J. Nucl. Mater. 307–311 (2002) 547.
[5] D.L. Smith, M.C. Billone, K. Natessan, Int. J. Refract. Met. Hard Mater. 18 (2000) 213.
[6] X. Liu, T. Yamada, Y. Yamauchi, Y. Hirohata, T. Hino, N. Noda, Fusion Eng. Des. 70 (2004) 329.
[7] Y. Hirohata, T. Yamada, Y. Yamauchi, T. Hino, T. Nagasaka, T. Muroga, J. Nucl. Mater. 348 (2006) 33.
[8] Y. Hirohata, T. Yamada, Y. Yamauchi, T. Hino, T. Nagasaka, T. Muroga, Fusion Eng. Des. 81 (2006) 193.
[9] A.V. Fedorov, A. van Veen, A.I. Ryazanov, J. Nucl. Mater. 258–263 (1998) 1396.
[10] A.V. Fedorov, A. van Veen, A.I. Ryazanov, J. Nucl. Mater. 233–237 (1996) 385.
[11] A. van Veen, A.V. Fedorov, A.I. Ryazanov, J. Nucl. Mater. 258–263 (1998) 1400.
[12] M. Fjiwara, K. Takanashi, M. Satou, A. Hasegawa, K. Abe, K. Kakiuchi, T. Furuya, J. Nucl. Mater. 329–333 (2004) 452.
[13] T. Muroga, T. Nagasaka, A. Iiyoshi, A. Kawabata, S. Sakurai, M. Sakata, J. Nucl. Mater. 283–287 (2000) 711.
[14] Y. Yamauchi, T. Hino, K. Koyama, Y. Hirohata, T. Yamashina, J. Nucl. Mater. 241–243 (1997) 1016.
[15] N. Matsunami, Y. Yamamura, et al., Nucl. Data table 31 (1) (1984) 26.
[16] P.A. Redhead, Vacuum 12 (1962) 203.